AD-A266 717 AGE

Form Approved
OMB No. 0704-0188

Public reporting burden for this collection of information is estimated to average 1 hour per response, including the time for reviewing instructions, searching existing data sources, gathering and maintaining the data needed, and completing and reviewing the collection of information. Send comments regarding this burden estimate or any other aspect of this collection of information, including suggestions for reducing this burden, to Washington Headquarters Services, Directorate for Information Operations and Reports, 1215 Jefferson Davis Highway, Suite 1204, Arlington, VA 22202-4302, and to the Office of Management and Budget, Paperwork Reduction Project (0704-0188), Washington, DC 20503.

1. AGENCY USE ONLY (Leave blank)	3. REPORT TYPE AND DATES COVERED
	Reprint June 1993

4. TITLE AND SUBTITLE
Phosphine Chemistry on Mo(110) and Oxidized Mo(110)

5. FUNDING NUMBERS
DAAL03-91-G-0323

6. AUTHOR(S)
X. Zhang, A. Linsebigler, U. Heiz, and J.T. Yates, Jr.

7. PERFORMING ORGANIZATION NAME(S) AND ADDRESS(ES)
University of Pittsburgh
Surface Science Center
Pittsburgh PA 15260

DTIC ELECTE JUL 9 1993 S C D

8. PERFORMING ORGANIZATION REPORT NUMBER

9. SPONSORING / MONITORING AGENCY NAME(S) AND ADDRESS(ES)
U.S. Army Research Office
P. O. Box 12211
Research Triangle Park, NC 27709-2211

10. SPONSORING / MONITORING AGENCY REPORT NUMBER
ARO 29227.5-CH

11. SUPPLEMENTARY NOTES
The view, opinions and/or findings contained in this report are those of the author(s) and should not be construed as an official Department of the Army position, policy, or decision, unless so designated by other documentation.

12a. DISTRIBUTION / AVAILABILITY STATEMENT
Approved for public release; distribution unlimited.

12b. DISTRIBUTION CODE

13. ABSTRACT *(Maximum 200 words)*

93-15512

93 7 08 094

The adsorption and desorption of phosphine and the oxidation of phosphorus on Mo(110) and oxidized Mo(110) have been studied by using Auger electron spectroscopy (AES), temperature-programmed desorption (TPD), and low-energy electron diffraction (LEED). Both molecular desorption and dissociative processes were observed on Mo(110), leaving adsorbed P(a) species in a c(4×1) overlayer structure. The P(a) species do not undergo diffusion into the bulk below 1000 K. On the oxidized Mo(110) surface, the phosphine adsorption and dissociation process was inhibited significantly. Phosphorus on the Mo(110) surface could be oxidized to produce PO(g) and PO_2(g) species near 900 K, as detected by line-of-sight mass spectrometry; neither P_2O_3(g) nor P_2O_5(g) was observed.

14. SUBJECT TERMS		15. NUMBER OF PAGES
Phosphorus	Molybdenum	
Phosphine	Catalysis	16. PRICE CODE
Oxidation		

17. SECURITY CLASSIFICATION OF REPORT	18. SECURITY CLASSIFICATION OF THIS PAGE	19. SECURITY CLASSIFICATION OF ABSTRACT	20. LIMITATION OF ABSTRACT
UNCLASSIFIED	UNCLASSIFIED	UNCLASSIFIED	UL

DISCLAIMER NOTICE

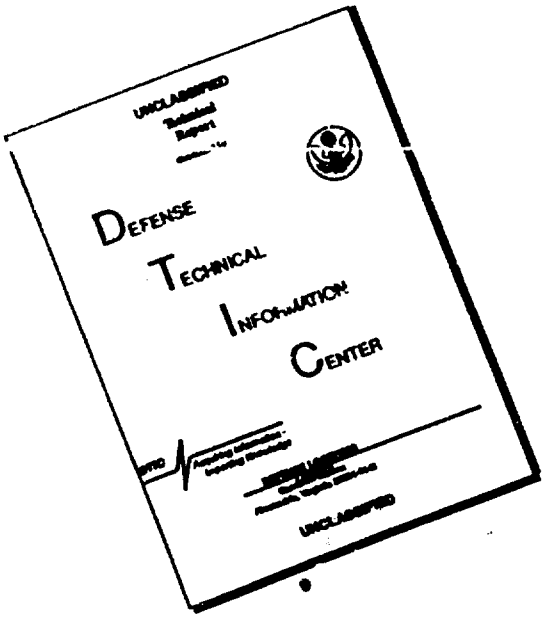

THIS DOCUMENT IS BEST QUALITY AVAILABLE. THE COPY FURNISHED TO DTIC CONTAINED A SIGNIFICANT NUMBER OF PAGES WHICH DO NOT REPRODUCE LEGIBLY.

Reprinted from The Journal of Physical Chemistry, 1993, 97.

Phosphine Chemistry on Mo(110) and Oxidized Mo(110)

X. Zhang, A. Linsebigler, U. Heiz, and J. T. Yates, Jr.*

Surface Science Center, Department of Chemistry, University of Pittsburgh, Pittsburgh, Pennsylvania 15260

Received: July 6, 1992; In Final Form: January 15, 1993

The adsorption and desorption of phosphine and the oxidation of phosphorus on Mo(110) and oxidized Mo(110) have been studied by using Auger electron spectroscopy (AES), temperature-programmed desorption (TPD), and low-energy electron diffraction (LEED). Both molecular desorption and dissociative processes were observed on Mo(110), leaving adsorbed P(a) species in a c(4×1) overlayer structure. The P(a) species do not undergo diffusion into the bulk below 1000 K. On the oxidized Mo(110) surface, the phosphine adsorption and dissociation process was inhibited significantly. Phosphorus on the Mo(110) surface could be oxidized to produce PO(g) and PO_2(g) species near 900 K, as detected by line-of-sight mass spectrometry; neither P_2O_3(g) nor P_2O_5(g) was observed.

I. Introduction

Certain phosphorus compounds used in pesticides, herbicides, and chemical agents are extremely hazardous materials. Degradation of these chemicals into less harmful substances using heterogeneous catalytic methods is therefore of great importance.[1] The surface chemistry of phosphine and organophosphorus compounds has been studied on both single-crystal metals and semiconductors[2-4] and on supported metal catalysts[5] and oxides.[6-8] The decomposition and oxidation of the organophosphorus compound dimethyl methylphosphonate on certain single-crystal surfaces, Ni(111),[9] Pd(111),[9] Mo(110),[10] and Pt(111),[11] have also been investigated. Studies on Mo(110) and Pd(111) showed that the rate-limiting surface process to establish a continuous oxidation reaction was the regeneration of catalytically active sites which were free of chemisorbed phosphorus. Phosphorus is removed by the production of volatile phosphorus oxides. On this basis, we have selected the catalytic oxidation of elemental phosphorus as a key issue for study. The oxidation of phosphine has also been studied recently on a supported MoO_3 catalyst.[12] Here, infrared spectroscopy was used to observe surface intermediates present in the oxidation process, and a final stage of phosphorus oxide desorption was observed at about 800 K.

As part of the continuing systematic comparative study of phosphorus oxidation on a variety of transition metals and oxides, this paper reports the study of the oxidation of elemental phosphorus on a Mo(110) single crystal and also on MoO_x thin films prepared by adsorbing oxygen on Mo(110) at high temperature. A related study of the surface chemistry of phosphine on Mo(110) is also presented here.

II. Experimental Section

The experiments were performed in a stainless steel ultrahigh-vacuum system described in detail previously.[13] The typical system base pressure was less than 1×10^{-10} mbar. The ultrahigh-vacuum chamber is equipped with a differentially pumped and digitized quadrupole mass spectrometer (QMS) for temperature-programmed desorption (TPD), a cylindrical mirror analyzer (CMA) for Auger electron spectroscopy (AES), low-energy electron diffraction (microchannel plate amplifier, LEED), and two calibrated and collimated capillary array dosers. The QMS was located in a differentially pumped shield containing a 1.6-mm-diameter aperture. This arrangement permits study of temperature-programmed desorption from the front face of the Mo(110) crystal by line-of-sight detection using the mass spectrometer.

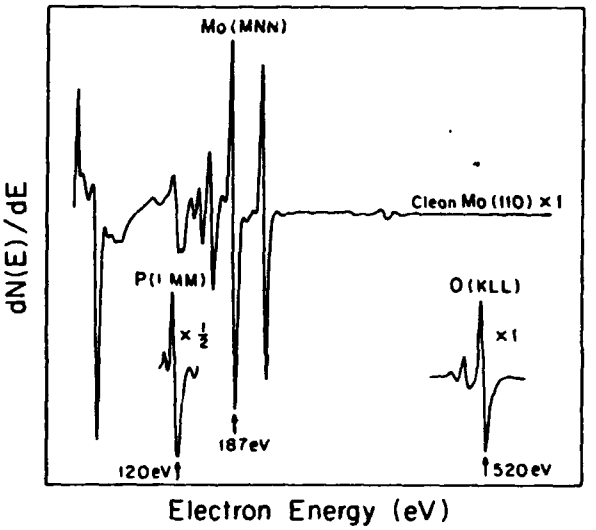

Figure 1. Auger spectrum of the clean Mo(110) single crystal. Also shown are the phosphorus Auger peak for saturated phosphorus on the surface and the oxygen peak for MoO_x (y = O/Mo Auger ratio = 0.3).

The Mo(110) single crystal (12-mm diameter × 2-mm thickness) was polished with standard techniques and oriented within 1° of the (110) direction by Laue back-reflection X-ray diffraction. It had two 0.35-mm slots cut into the top and bottom for mounting. Resistive heating of the 0.35-mm-diameter tungsten wires held in the slots led to crystal heating by conduction. The crystal temperature was measured by a chromel-alumel thermocouple spot-welded to the back of the crystal. A linear heating rate (1.1 K/s) was achieved with an electronic temperature programmer.[14]

The initial crystal cleaning procedure is described elsewhere.[10] Each day the crystal was cleaned by cycles of oxygen treatment at 1100 K (carbon removed) and Ar^+ sputtering (1 keV, 1100 K) (O, P, and S removed) followed by annealing to 1200 K in vacuum.

These procedures produced a clean Mo(110) surface within the detection limit of AES, and a sharp (1 × 1) LEED pattern was obtained after these procedures. The Auger spectrum of the clean Mo(110) is shown in Figure 1. The surface was considered to be free of sulfur when the [Mo + S](151 eV)/Mo(187 eV) ratio reached a steady value of 0.16 and was considered to be free of phosphorus when the [Mo + P](120 eV)/Mo(187 eV) ratio reached a steady value of 0.21. The values of the P(120 eV)/Mo(187 eV) ratio reported in this paper were obtained from the

0022-3654/93/2097-5074$04.00/0

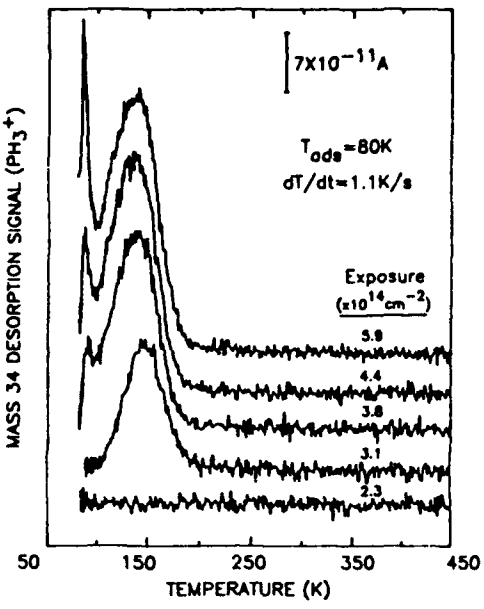

Figure 2. Temperature-programmed desorption spectra of PH_3 on Mo(110) as a function of exposure. dT/dt = 1.1 K/s.

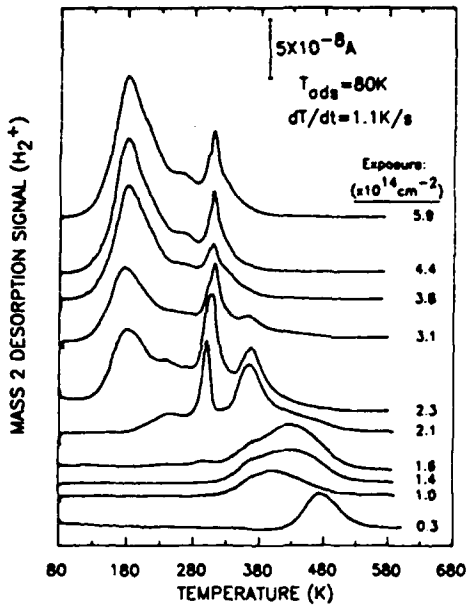

Figure 3. Temperature-programmed desorption spectra of H_2 from dissociatively adsorbed PH_3 on Mo(110) as a function of exposure. dT/dt = 1.1 K/s.

difference between the measured [Mo + P](120 eV)/Mo(187 eV) value and 0.21.

Phosphine and deuterium gas were dosed to the crystal surface through a calibrated microcapillary array collimated beam doser.[15-18] The doser axis was oriented normal to the surface and delivered a flux of 3.19×10^{12} $PH_3/(cm^2\ s)$ to the surface when the gas line pressure was 0.5 Torr. At the crystal position 12 mm from the doser, a geometrical interception factor of 0.3 was employed[16,17] to calculate the flux received by the crystal. In the phosphorus oxidation experiment, oxygen was delivered to the system through a leak valve to a steady system pressure in the 10^{-8}–10^{-5} mbar range while the crystal was positioned and heated in front of the QMS.

Phosphine was obtained from Matheson Gas Products (99.9% pure). Three freeze–pump–thaw cycles were performed before it was used. Deuterium was obtained from Cambridge Isotope Laboratories (D, 99.8% pure).

III. Results

Auger Spectroscopy Studies of P/Mo(110). Figure 1 shows the Auger spectrum of a clean Mo(110) single crystal. Also shown are the P(*LMM*) peak after phosphine decomposition and the O(*KLL*) peak of MoO_x (O(520 eV)/Mo(187 eV) ratio y = 0.3). It was found from P/Mo Auger ratios that the surface phosphorus did not diffuse into the Mo(110) crystal in the temperature range 600–1000 K. This result differs from studies on P/Pt(111)[3a] where surface phosphorus diffused into the bulk at 600–900 K. An analysis of the Auger intensity ratios suggests that an atom ratio P/Mo of about 0.4 exists in the depth of Auger sampling for the PH_3 saturated surface. In addition, it was found that electron irradiation (3.0 kV, 8×10^{17} e/cm²) did not result in preceptible loss of surface phosphorus by electron-stimulated desorption, indicating that Auger spectroscopy was not a perturbing probe for measurements of phosphorus surface coverage.

Adsorption and Desorption of PH_3. A series of TPD experiments were performed for different PH_3 exposures at 80 K. Adsorbed phosphine was partially desorbed, and partially dissociated, producing P(a) and H(a). H(a) desorbed as H_2, and phosphorus was left on the surface of the crystal after heating. Figure 2 shows phosphine TPD spectra from the Mo(110) surface for increasing exposure to phosphine. At low exposures, there was no phosphine desorption. All of the phosphine decomposed completely either upon adsorption at 80 K or upon heating. At intermediate exposures, only one phosphine desorption state was detected. This desorption state was due to the first layer of chemisorbed phosphine. At higher exposures, a low-temperature shoulder (85 K) developed; it originates from multilayer physisorbed phosphine.

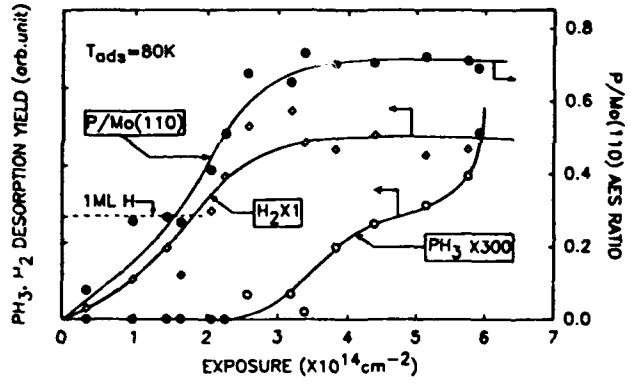

Figure 4. PH_3 decomposition and desorption yields as a function of PH_3 exposure. Desorption yields are calculated from total desorption peak areas. The saturation coverage of H was measured from H_2 desorption from clean Mo(110) and is designated 1 ML in the figure.

Figure 3 shows a set of hydrogen desorption spectra from the TPD of dissociatively adsorbed PH_3 on Mo(110) for increasing PH_3 exposure. At low PH_3 exposures, the hydrogen desorption behavior was similar to that for hydrogen desorption from clean Mo(110).[19] As the PH_3 exposure was increased, two other low-temperature H_2 desorption states developed. When the lowest-temperature H_2 desorption state reached saturation, the maximum amount of phosphorus on the surface (θ_P^{rel} = 1) was obtained. Figure 3 also indicates that at higher coverages phosphine began to dissociate at a temperature of 120 K or lower, yielding hydrogen. The saturated hydrogen desorption yield from PH_3 adsorption was 1.77 ± 0.06 times greater than for pure hydrogen desorption from a hydrogen monolayer on clean Mo(110).

The effect of preadsorbed phosphorus on hydrogen adsorption on Mo(110) was studied at monolayer P coverage. Only the highest-temperature H_2 desorption state was detected and amounted to 5% of the saturated coverage of hydrogen from PH_3.

Figure 4 shows the desorption yield of H_2 and PH_3 as a function of PH_3 exposure. In addition, the buildup of the phosphorus

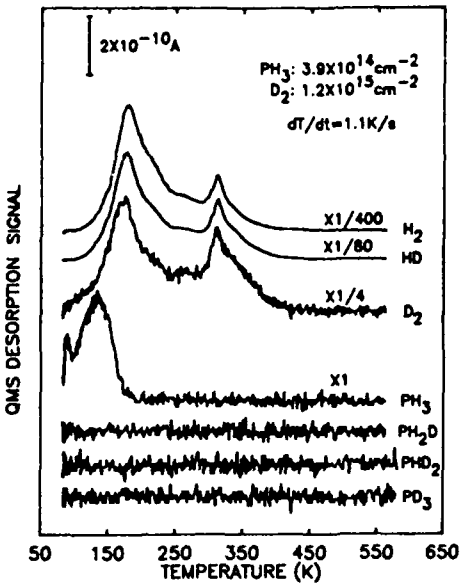

Figure 5. Temperature-programmed desorption spectra following deuterium and phosphine coadsorption on Mo(110). A mixture of deuterium and phosphine at the same gas line partial pressure was used.

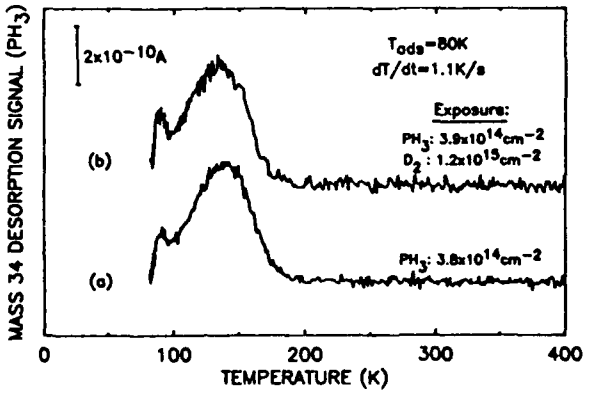

Figure 6. Comparison of PH_3 TPD spectra from PH_3/Mo(110) and from PH_3/D_2/Mo(110).

Auger signal for increasing PH_3 exposures is shown. Auger spectra were taken after each TPD measurement. This figure indicates that at low exposures all of the phosphine is dissociated upon adsorption or heating. When the phosphine exposure is increased, the dissociation of PH_3 reached saturation (at an exposure of about 4×10^{14} PH_3 cm^{-2}), and additional adsorbed PH_3 desorbs nondissociatively as PH_3. The three measurements conform to each other. Both the H_2 desorption yield and the P/Mo Auger ratio reached saturation at an exposure to PH_3 of about 4×10^{14} PH_3 cm^{-2}, and a little below this saturation exposure, phosphine began to desorb.

Isotopic Exchange Studies. To better understand phosphine adsorption and desorption on Mo(110), an isotope-exchange experiment was performed. Deuterium and phosphine at the same partial pressure were mixed in the gas line. Temperature-programmed desorption was carried out after the mixed gas was adsorbed on Mo(110) at 80 K. The result of this deuterium and phosphine coadsorption experiment is displayed in Figure 5. All the possible deuterium isotope-exchange products were monitored. For phosphine desorption, only PH_3 was detected. Neither PH_2D, PHD_2, nor PD_3 was produced. For hydrogen desorption, all of the isotopically labeled hydrogen molecules were observed. This experiment indicates clearly that neither P(a) nor PH_x(a) recombines with D(a) to produce isotopically labeled phosphine molecules.

A comparison of phosphine desorption from PH_3/Mo(110) and from PH_3/D_2/Mo(110) was made, and the result is shown in Figure 6. Coadsorbed deuterium had no effect on the phosphine desorption kinetics. In addition, the preadsorption of deuterium does not diminish the retention of P(a) from PH_3 decomposition on Mo(110).

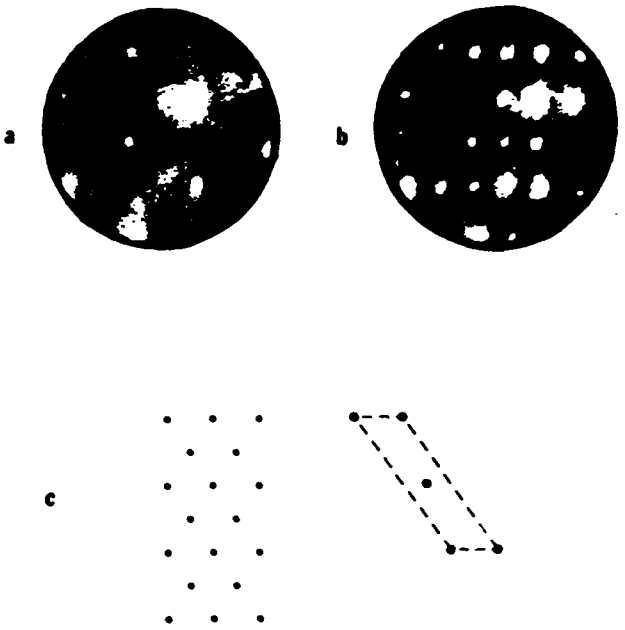

Figure 7. (a) LEED pattern of clean Mo(110). (b) LEED pattern of P/Mo(110). (c) c(4×1) P overlayer structure compared to the unreconstructed Mo(110) surface. The P overlayer was produced from a saturated PH_3 layer.

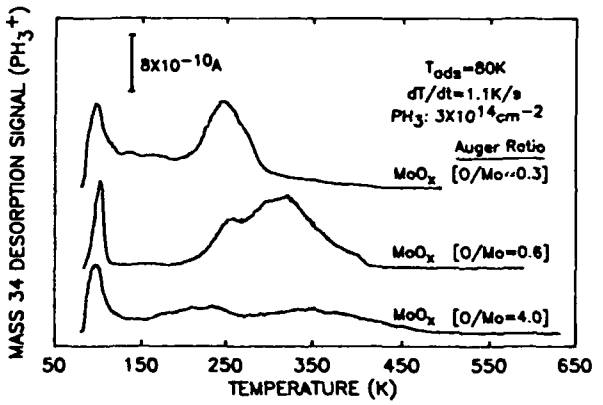

Figure 8. Temperature-programmed desorption spectra of PH_3 on various MoO_x thin films. The y values, [O/Mo], are O(520 eV)/Mo(187 eV) Auger peak-to-peak ratios.

LEED Studies of P/Mo(110). LEED experiments were also performed. Adsorption of saturated PH_3 at 80 K produced no extra LEED beams. After heating the crystal with saturated PH_3 to 600–1000 K to leave only P(a) on the crystal, a c(4×1) LEED pattern was observed. This indicates that phosphorus is ordered on Mo(110). Figure 7 shows the LEED patterns observed in these experiments and the phosphorus overlayer structure. A c(4×1) structure corresponds to a coverage of 0.5 P atom/Mo atom.

Adsorption and Desorption of Phosphine on MoO_x. Molybdenum oxide layers were produced by exposing the Mo(110) crystal at 1000 K to O_2(g). Auger spectroscopy was used to measure the surface composition. One monolayer of molybdenum oxide was produced when the O/Mo(110) ratio was 0.3 (y = 0.3).[20] An oriented oxide layer was produced when the O(520 eV)/Mo(187 eV) Auger ratio was 0.6 (y = 0.6). A much thicker molybdenum oxide layer (y = 4.0) was also prepared.

Temperature-programmed desorption spectra for PH_3 from three different molybdenum oxide layers are shown in Figure 8.

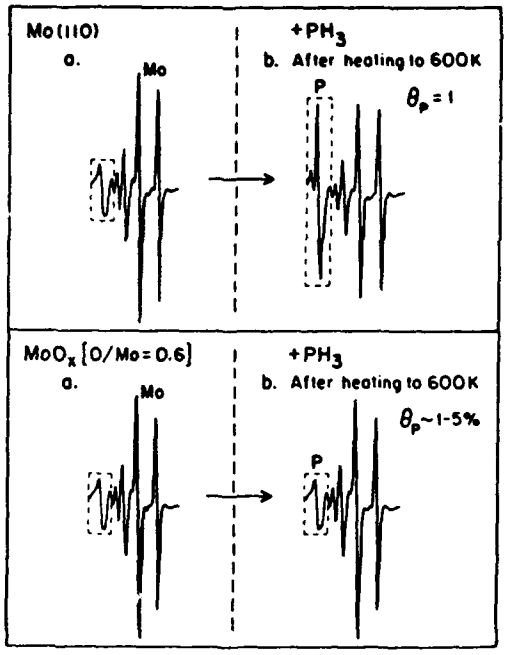

Figure 9. Auger spectra taken before phosphine adsorption and after phosphine desorption on Mo(110) and MoO_x (y = 0.6) thin film. The PH_3 exposure was 3.8×10^{14} PH_3/cm^2.

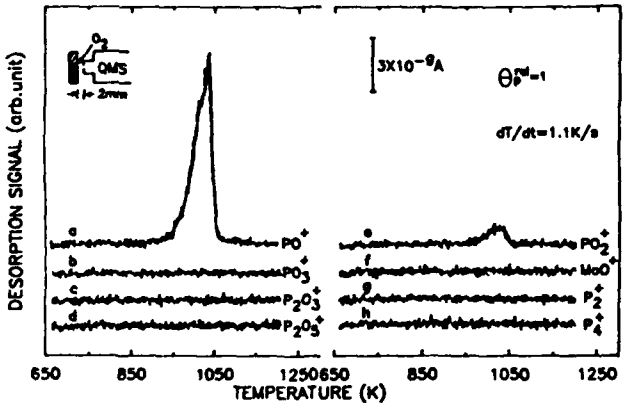

Figure 10. Phosphorus oxidation on Mo(110) in 1.0×10^{-5} mbar of O_2. The masses monitored were (a) 47, (b) 79, (c) 110, (d) 142, (e) 63, (f) 112, (g) 62, and (h) 124 amu.

On all the MoO_x layers, the phosphine decomposition was inhibited as was observed for phosphine on iron oxide.[6a] On one monolayer of MoO_x (y = 0.3), the phosphine decomposition is only 20% of that on Mo(110) as measured by the P/Mo Auger ratio taken after heating. In this case (y = 0.3), besides phosphine, some hydrogen desorption was also detected. Only phosphine desorption was detected for the thicker molybdenum oxide layer. The chemisorbed PH_3 desorption maximum was shifted to higher temperatures (as the molybdenum oxide layer thickness increased) compared to phosphine desorption from Mo(110). The phosphine desorption kinetics were different on the different oxide layers as displayed in Figure 8.

The adsorption of phosphine on the oriented MoO_x films (y = 0.6 and y = 4.0) was further investigated by Auger electron spectroscopy. Figure 9 shows the AES of Mo(110) and MoO_x (y = 0.6) taken before phosphine adsorption and after phosphine thermal desorption. After phosphine desorption, the phosphorus retained on the MoO_x film was only 1–5% of that retained on Mo(110). This indicates that phosphine decomposition on the oriented molybdenum oxide layers was inhibited extensively below 600 K.

The desorption of H_2O from PH_3/MoO_x layers was not detected by line-of-sight mass spectrometry.

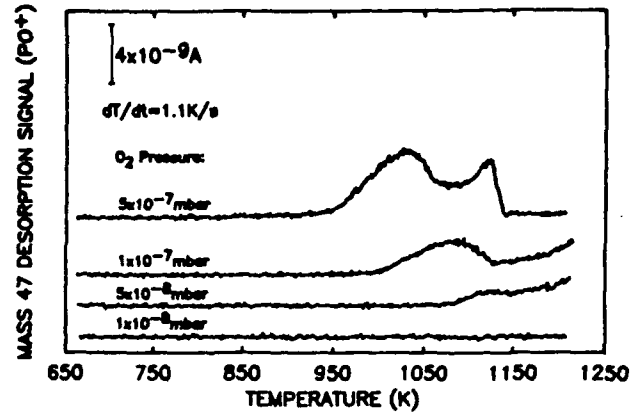

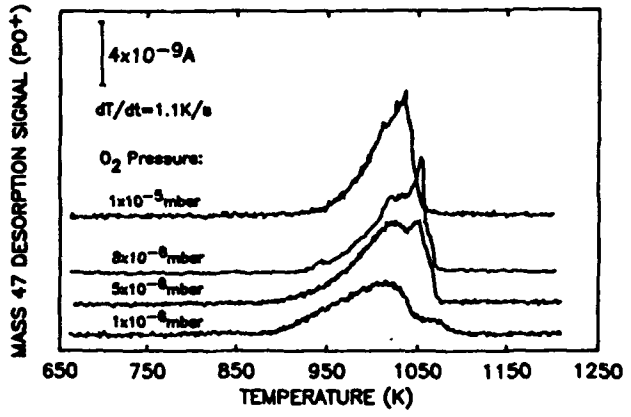

Figure 11. Phosphorus oxidation in an O_2 environment at different pressures. A saturated phosphorus layer was present on the surface. Oxygen was admitted to the chamber to the desired steady pressure.

Phosphorus Oxidation on Mo(110) and MoO_x (y = 0.3). Phosphorus oxidation experiments were performed by programmed heating of the crystal, containing a saturated phosphorus layer, in an oxygen background pressure while monitoring desorbed species from the surface by line-of-sight mass spectrometer measurements. Different oxygen pressures (1×10^{-8} to 1×10^{-5} mbar) were used. MoO^+, P_2^+, P_4^+ and several kinds of phosphorus oxides were monitored. Only PO^+ and PO_2^+ were detected near 1050 K as shown in Figure 10. Because PO_3^+, $P_2O_3^+$, and $P_2O_5^+$ were not detected, the desorption species could only be PO and/or PO_2 according to the phosphorus oxides' cracking patterns.[21] The desorption products are designated as PO_x.

A detailed study of phosphorus oxidation was carried out at various oxygen pressures. Phosphorus on the surface was converted to volatile oxides by temperature programming, and the desorption spectra yielding PO^+ in the mass spectrometer are shown in Figure 11. From the spectra, a trend could be seen indicating that phosphorus on Mo(110) could be removed from the surface completely by oxidation if the surface temperature was high enough. During the experiments the Mo(110) crystal was heated up to 1210 K, and at oxygen pressures higher than 5×10^{-7} mbar, phosphorus was removed completely. Auger spectra indicated that there was no phosphorus left on the surface after these oxidation procedures. The phosphorus oxide yields (monitored as PO^+) as a function of steady-state oxygen pressure are plotted in Figure 12. Here two PO_x desorption measurements at lower oxygen pressures are incomplete, as indicated by arrows, since some PO_x species desorb above 1210 K.

The TPD spectra in Figure 11 indicate that there are two PO_x desorption processes. Both processes shift to lower temperature when the O_2 pressure is increased from 1×10^{-8} to 1×10^{-6} mbar. The lowest onset temperature for PO_x desorption from the Mo(110) single crystal was 900 K in 1×10^{-6} mbar of oxygen.

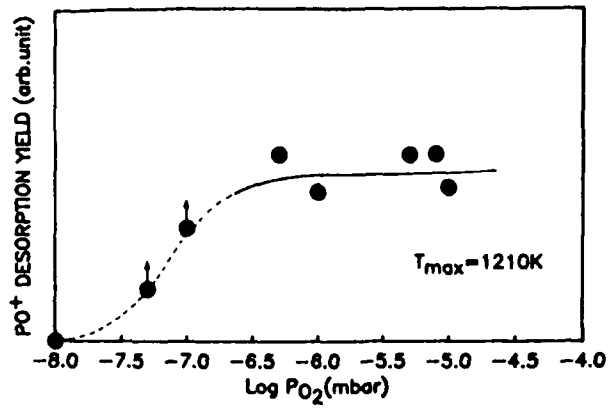

Figure 12. PO^+ desorption yield as a function of oxygen pressure. The Mo(110) crystal was heated to 1210 K.

IV. Discussion

Phosphine Adsorption on Mo(110): Coverage Estimations. The basis for an estimation of the absolute saturation phosphine coverage on Mo(110) is related to the measured yield of hydrogen from the decomposed PH_3. Estimations of the saturation coverage of pure hydrogen on Mo(110) range from 0.86×10^{15} to 1.73×10^{15} cm^{-2}.[22] It is noted that this upper limit for hydrogen absolute coverage corresponds to 1.2 H/Mo and is probably unrealistic.

We measured that the ratio of hydrogen evolution from a saturated PH_3 layer to pure hydrogen (saturated) is 1.77 ± 0.06. This implies that the PH_3 saturation coverage is in the range 0.51×10^{15} to 1.02×10^{15} cm^{-2}. Therefore, based on the hydrogen yield from saturated PH_3, the phosphorus coverage ranges from 0.36 P/Mo to 0.73 P/Mo, using a Mo atom surface density of 1.4×10^{15} cm^{-2} in the unreconstructed Mo(110) surface.

The c(4×1) LEED pattern obtained for the P overlayer produced from the saturated PH_3 corresponds to 0.5 P/Mo, well within the large range of the saturated absolute P coverage, based on H_2 yield measurements.

From Figure 4, it may be seen that an exposure of about 4×10^{14} PH_3/cm^2 leads to PH_3 saturation as judged by the yield of the hydrogen. This agrees fairly well with the lower estimate of the PH_3 saturation coverage (about 5×10^{14} PH_3 cm^{-2}) and is consistent with the lower estimate of the saturation coverage of pure hydrogen on Mo(110)[22,23] and also approximately with the LEED measurement (0.7×10^{15} P/cm^2).

Phosphine Bonding to Mo(110). The bond between phosphine and a metal can be compared to that between CO and a metal. The phosphorus lone pair electrons act as an electron pair donor to Mo acceptor atoms, enabling the phosphorus atom in PH_3 to adopt a pseudotetrahedral configuration on atop Mo sites. In addition to acting as a σ donor, however, phosphine can act as a π electron acceptor when vacant 3d orbitals of phosphorus interact with nonbonding orbitals of a transition metal, thus increasing the metal–P bond strength. By analogy to PH_3 bonding in organometallic compounds, PH_3 binding to atop Mo(110) sites is assumed. The above argument is traditional for PH_3 bonding to a transition metal. It has been suggested recently that P–H σ^* orbitals participate in the π acceptor process for PH_3 bonding.[24]

Phosphine Desorption on Mo(110). An analysis of the desorption kinetics of the high-temperature PH_3 desorption state with peak maximum at 148 K (Figure 2) yields an extremely low activation energy and preexponential factor which is unrealistic for first-order desorption kinetics for PH_3 with a coverage-independent heat of adsorption. A large half-width (about 44 K) for the PH_3 desorption process is observed. In contrast, the sharp desorption feature at 84 K exhibits more normal desorption kinetics as judged by its small half-width, although the desorption kinetic order (zero or first order) cannot be determined from these data.

The unrealistic desorption kinetic behavior seen for the 148 K PH_3 desorption process may be due to repulsive PH_3–PH_3 interactions in the overlayer, causing a significant coverage-dependent shift in the activation energy for desorption. Similar effects, due to repulsive dipole–dipole interactions, have been observed for NH_3 on Ru(001).[25]

From the D(a) + PH_3(a) coadsorption experiment, coadsorbed deuterium had no effect on PH_3 desorption, as shown in Figure 6, nor on the coverage of P(a) produced by PH_3(a) decomposition. This suggests that deuterium adsorbs on different sites from PH_3. Hydrogen is assumed to adsorb in the Mo(110) hollow sites, whereas PH_3 is adsorbed on terminal sites of Mo(110). Also, from the deuterium isotope exchange experiment (Figure 5), we found that molecular phosphine desorption (about 148 K) did not occur via a recombination process, again suggesting that PH_3(a) and H(a) behave independently on Mo(110).

PH_3 Adsorption on MoO_x. A comparison between the thermal desorption results for PH_3 on Mo(110) and PH_3 on MoO_x (Figures 2 and 8) indicates that MoO_x surfaces result in the desorption of PH_3 at higher temperatures than observed on Mo(110). Thus, the decomposition of PH_3 is retarded by surface oxygen and/or the bond between PH_3 and the surface is strengthened in the presence of surface oxygen. Figure 8 indicates that the bonding energy of PH_3 to MoO_x increases somewhat as x increases, ultimately leading to a broad PH_3 desorption state with the TPD peak maximum near 350 K.

Volatile Oxidation Products from PH_3 on Mo(110) and MoO_x. Only PO^+ and PO_2^+ are detected by the line-of-sight mass spectrometer during the catalytic oxidation of PH_3 (Figures 10–12). Because neither P_2O_3 nor P_2O_5 was detected, the volatile phosphorus oxide can only be PO_2(g) or a mixture of PO_2(g) and PO(g). The P_2O_3 or P_2O_5 mass spectrometer cracking pattern in ref 21 suggests that large relative intensities of $P_2O_5^+$ and/or $P_2O_3^+$ would have been detected if the neutral parent phosphorus oxide molecules were desorbed in this experiment. Both PO(g) and PO_2(g) are known molecules which are stable, and their thermodynamic properties have been evaluated from their spectra.[26]

V. Summary and Conclusions

The interaction of PH_3 with Mo(110) and MoO_x films on Mo(110) has been studied in the temperature range 80–1210 K. The following results have been found.

1. PH_3 adsorption on Mo(110) results in H_2 desorption at temperatures near 120 K at the highest PH_3 coverages. Thus, phosphine decomposition begins near or below 120 K on Mo(110), producing adsorbed P or PH_x species.

2. At high PH_3 exposures, the presence of undecomposed chemisorbed PH_3 was found on the basis of PH_3 thermal desorption in two low-temperature PH_3 desorption processes. Isotopic studies with D(a) + PH_3(a) indicate that neither exchange nor recombination reactions to produce PH_3(g) occur. In addition, preadsorbed deuterium does not diminish the capacity of Mo(110) to chemisorb PH_3.

3. No evidence for diffusion of adsorbed P into the Mo(110) bulk was obtained in the temperature range 600–1000 K.

4. The hydrogen thermal desorption was measured for various PH_3 exposures. Higher PH_3 coverages produce H_2 desorption at temperatures below that for pure H_2 desorption from Mo(110) as a result of a P(a)–H(a) repulsive interaction.

5. LEED studies of P/Mo(110) produced from the decomposition of a saturated PH_3 layer show the production of a c(4×1) overlayer, corresponding to 0.5 P/Mo. Studies of H_2 desorption from PH_3 and of the P/Mo Auger intensity indicate a saturation coverage range of PH_3 corresponding to 0.36–0.73 P/Mo, where only the decomposed PH_3 is measured in this case.

6. Phosphine dissociation on MoO_x films was inhibited compared to dissociation on the clean Mo(110). For a three-

dimensional MoO_x layer, only 1–5% of the P/Mo Auger ratio could be obtained by monolayer PH_3 decomposition compared to clean Mo(110). MoO_x layers retain undissociated PH_3 up to 350 K, whereas PH_3 desorption from Mo(110) is completed below 200 K.

7. Both PO^+ and PO_2^+ mass spectral cracking products were observed near 900 K during phosphorus oxidation over Mo(110) in O_2(g). Neither P_2O_3 nor P_2O_5 products are produced under the condition of this ultrahigh-vacuum experiment.

Acknowledgment. The authors gratefully acknowledge the financial support of the Army Research Office (Contract DAAL03-91-G-0323). Ueli Heiz acknowledges an Andrew Mellon Postdoctoral Fellowship from the University of Pittsburgh.

References and Notes

(1) Ekerdt, J. G.; Klabunde, K. J.; Shapley, J. R.; White, J. M.; Yates, J. T., Jr. *J. Phys. Chem.* **1988**, *92*, 6182.

(2) (a) Hegde, R. I.; Tobin, J.; White, J. M. *J. Vac. Sci. Technol. A3* (2), **1985**, 339. (b) Greenlief, C. M.; Hedge, R. I.; White, J. M. *J. Phys. Chem.* **1985**, *89*, 5681. (c) Hegde, R. I.; White, J. M. *Surf. Sci.* **1985**, *157*, 17. (d) Hegde, R. I.; Greenlief, C. M.; White, J. M. *J. Phys. Chem.* **1985**, *89*, 2886.

(3) (a) Mitchell, G. E.; Henderson, M. A.; White, J. M. *Surf. Sci.* **1987**, *191*, 425. (b) Henderson, M. A.; White, J. M. *J. Am. Chem. Soc.* **1988**, *110*, 6939. (c) Mitchell, G. E.; Henderson, M. A.; White, J. M. *J. Phys. Chem.* **1987**, *91*, 3808.

(4) Chen, P. J.; Colaianni, M. L.; Wallace, R. M.; Yates, J. T., Jr. *Surf. Sci.* **1991**, *244*, 177.

(5) (a) Lu, G.; Darwell, J. E.; Crowell, J. E. *J. Phys. Chem.* **1990**, *94*, 8326. (b) Lu, G.; Crowell, J. E. *J. Phys. Chem.* **1990**, *94*, 5644.

(6) (a) Hegde, R. I.; White, J. M. *J. Phys. Chem.* **1986**, *90*, 2159. (b) Hegde, R. I.; White, J. M. *Surf. Sci. 28*, **1981**, 10.

(7) Henderson, M. A.; Jin, T.; White, J. M. *J. Phys. Chem.* **1986**, *90*, 4607.

(8) (a) Templeton, M. K.; Weinberg, W. H. *J. Am. Chem. Soc.* **1985**, *107*, 97. (b) *Ibid.* **1985**, *107*, 774.

(9) Guo, X.; Yoshinobu, J.; Yates, J. T., Jr. *J. Phys. Chem.* **1990**, *94*, 6839.

(10) Smentkowski, V. S.; Hagans, P.; Yates, J. T., Jr. *J. Phys. Chem.* **1988**, *92*, 6351.

(11) Henderson, M. A.; White, J. M. *J. Am. Chem. Soc.* **1988**, *110*, 6939.

(12) Paul, D. K.; Rao, L. F.; Yates, J. T., Jr. *J. Phys. Chem.* **1992**, *96*, 3446.

(13) Gates, S. M.; Russell, J. N., Jr.; Yates, J. T., Sr. *Surf. Sci.* **1985**, *159*, 233.

(14) Muha, R. J.; Gates, S. M.; Basu, P.; Yates, J. T., Jr. *Rev. Sci. Instrum.* **1985**, *56* (4), 613.

(15) Bozack, M. J.; Muehlhoff, L.; Russell, J. N., Jr.; Choyke, W. J.; Yates, J. T., Jr. *J. Vac. Sci. Technol.* **1987**, *A5*, 1.

(16) Campbell, C. T.; Valone, S. M. *J. Vac. Sci. Technol.* **1985**, *13*, 408.

(17) Winkler, A.; Yates, J. T., Jr. *J. Vac. Sci. Technol.* **1988**, *A6* (5), 2929.

(18) Smentkowski, V. S.; Yates, J. T., Jr. *J. Vac. Sci. Technol. A7* (6), **1989**, 3325.

(19) Ernst-Vidalis, M.-L.; Kamaratos, M.; Papageorgopoulos, C. *Surf. Sci.* **1987**, *189/190*, 276.

(20) Colaianni, M. L.; Chen, J. G.; Weinberg, W. H.; Yates, J. T., Jr. *Surf. Sci.* **1992**, *279*, 211.

(21) Muenow, D. W.; Uy, O. M.; Margrave, J. L. *J. Inorg. Nucl. Chem.* **1970**, *32* (11), 3459.

(22) Mahnig, M.; Schmidt, L. D. *Z. Phys. Chem.* (*Munich*) **1972**, *80*, 71. It should be pointed out that the estimation of absolute hydrogen coverage on Mo(110) and on related W single crystals is of poor accuracy. The saturation coverage of the primary standard (W(100)) is reported to be 1.5×10^{15} H/cm^2 by Tamm and Schmidt (Tamm, P.; Schmidt, L. D. *J. Chem. Phys.* **1971**, *54*, 4775). A second measurement by Madey (Madey, T. E. *Surf. Sci.* **1973**, *36*, 281) reports 2.0×10^{15} H/cm^2 on W(100). Tamm and Schmidt estimated that errors of a factor of 2 in saturation hydrogen coverage may exist in their comparison of different crystals with W(100). Thus, for Mo(110) the range of saturation hydrogen coverage is 0.86×10^{15} to 1.73×10^{15} H cm^{-2}.

(23) Tamm, P.; Schmidt, L. D. *J. Chem. Phys.* **1971**, *54*, 4775.

(24) (a) Corbridge, D. E. C. *The Structural Chemistry of Phosphorus*; Elsevier Scientific Publishing: New York, 1974; p 6. (b) Xiao, S.-X.; Trogler, W. C.; Ellis, D. E.; Berkovitch-Yellin, Z. *J. Am. Chem. Soc.* **1983**, *105*, 7033. (c) Orpen, A. G.; Connelly, N. G. *J. Chem. Soc., Chem. Commun.* **1985**, 1310. (d) Orpen, A. G.; Connelly, N. G. *Organometallics* **1990**, *9*, 1206. (e) Marynick, D. S. *J. Am. Chem. Soc.* **1984**, *106*, 4064.

(25) Benndorf, C.; Madey, T. E. *Surf. Sci.* **1983**, *135*, 164.

(26) *J. Phys. Chem. Ref. Data* **1985**, *14* (Suppl. 1), 1642, 1670.